Secondary Structure and Interfacial Aggregation of Amyloid-β(1−40) on Sodium Dodecyl Sulfate Micelles[†]

Vijayaraghavan Rangachari, Dana Kim Reed, Brenda D. Moore, and Terrone L. Rosenberry*

Department of Neuroscience, Mayo Clinic College of Medicine, 4500 San Pablo Road, Jacksonville, Florida 32224

Received February 15, 2006; Revised Manuscript Received May 16, 2006

ABSTRACT: Alzheimer's disease (AD) is characterized by the presence of large numbers of fibrillar amyloid deposits in the form of senile plaques in the brain. The fibrils in senile plaques are composed of 40- and 42-residue amyloid-β (Aβ) peptides. Several lines of evidence indicate that fibrillar Aβ and especially soluble Aβ aggregates are important in the pathogenesis of AD, and many laboratories have investigated soluble Aβ aggregates generated from monomeric Aβ in vitro. Of these in vitro aggregates, the best characterized are called protofibrils. They are composed of globules and short rods, show primarily β-structure by circular dichroism (CD), enhance the fluorescence of bound thioflavin T, and readily seed the growth of long fibrils. However, one difficulty in correlating soluble Aβ aggregates formed in vitro with those in vivo is the high probability that cellular interfaces affect the aggregation rates and even the aggregate structures. Reports that focus on the features of interfaces that are important in Aβ aggregation have found that amphiphilic interactions and micellar-like Aβ structures may play a role. We previously described the formation of Aβ(1−40) aggregates at polar−nonpolar interfaces, including those generated at microdroplets formed in dilute hexafluoro-2-propanol (HFIP). Here we compared the Aβ(1−40) aggregates produced on sodium dodecyl sulfate (SDS) micelles, which may be a better model of biological membranes with phospholipids that have anionic headgroups. At both HFIP and SDS interfaces, changes in peptide secondary structure were observed by CD immediately when Aβ(1−40) was introduced. With HFIP, the change involved an increase in predominant β-structure content and in fluorescence with thioflavin T, while with SDS, a partial α-helical conformation was adopted that gave no fluorescence. However, in both systems, initial amorphous clustered aggregates progressed to soluble fibers rich in β-structure over a roughly 2 day period. Fiber formation was much faster than in the absence of an interface, presumably because of the close intermolecular proximity of peptides at the interfaces. While these fibers resembled protofibrils, they failed to seed the aggregation of Aβ(1−40) monomers effectively.

Alzheimer's disease (AD)[1] is characterized by the presence of large numbers of fibrillar amyloid deposits in the form of senile plaques in the brain (*1*). The fibrils in senile plaques are composed of 40- and 42-residue peptides (*2*, *3*), denoted Aβ(1−40) and Aβ(1−42), respectively, that are produced by cleavage of cellular amyloid precursor protein (APP) (*4*). The peptides are identical except for two additional amino acid residues (Ile and Ala) at the C-terminus of Aβ(1−42). As originally suggested by the amyloid cascade hypothesis (*5*), it appears likely that Aβ peptides and especially their aggregates initiate cellular events that lead to neurodegeneration and AD. The most striking evidence supporting this hypothesis comes from the identification of numerous mutations linked to early-onset familial AD (FAD) (*6*). All FAD mutations reported thus far increase either the overall level of production of Aβ, the level of the more amyloidogenic Aβ(1−42) relative to that of Aβ(1−40) (reviewed in ref *6*), or the propensity of a mutated Aβ to form amyloid aggregates (*7*).

A number of investigators now propose that soluble aggregates of Aβ, rather than monomers or insoluble amyloid fibrils, may be responsible for synaptic dysfunction in the brains of AD patients and AD animal models (*8*−*12*). These endogenous soluble Aβ aggregates are present at low levels, making their detection and characterization difficult, but certain species have been identified by SDS−PAGE and immunoblotting. Multiple Aβ bands of 4−12 kDa were observed in samples from AD brain (*13*), and similar bands were obtained from samples of Aβ immunoprecipitated from the conditioned medium of CHO cells that had been transfected with APP cDNA (*14*). The bands were identified as SDS-stable oligomers (primarily dimers and trimers) of monomeric (4 kDa) Aβ. The soluble Aβ species that give rise to these bands are of great interest, as they appear to potently inhibit hippocampal long-term potentiation (*15*) and disrupt cognitive function (*16*).

Better characterization of these soluble Aβ aggregates would be possible if they could be generated from monomeric Aβ in vitro. Two types of soluble Aβ aggregates have been described in vitro, protofibrils and oligomers, although

[†] This work was supported by Robert and Clarice Smith Fellowship awards (to V.R. and B.D.M.) and by an award from the American Heart Association, National Center (0535185N) to V.R.

* To whom correspondence should be addressed. Telephone: (904) 953-7375. Fax: (904) 953-7370. E-mail: rosenberry@mayo.edu.

[1] Abbreviations: AD, Alzheimer's disease; EM, electron microscopy; AFM, atomic force microscopy; APP, amyloid precursor protein; CD, circular dichroism; CMC, critical micelle concentration; DLS, dynamic light scattering; FAD, early-onset familial AD; HFIP, hexafluoro-2-propanol; SEC, size exclusion chromatography; SDS, sodium dodecyl sulfate; PAGE, polyacrylamide gel electrophoresis.

10.1021/bi060323t CCC: $33.50
Published on Web 06/22/2006

their structural correspondence to endogenous aggregates remains unclear. Protofibrils are formed by both Aβ(1−40) and Aβ(1−42) and meet established biophysical criteria. They exhibit Stokes radii of 10−50 nm as measured by dynamic light scattering (DLS) (*17*), show enhanced fluorescence with thioflavin T (*18*), give circular dichroism (CD) spectra that reveal β-structure (*18*), and display mixtures of roughly spherical globules, short, curly fibers (*17*, *19*, *20*), and short rods of 10−200 nm (*21*−*24*) by electron microscopy (EM) and atomic force microscopy (AFM). Protofibrils also readily grow to fibrils by elongation with Aβ monomer and by lateral association (*24*). A definition of oligomeric aggregates has been much more elusive, and some protofibril preparations have been called oligomers. About the only widely accepted criterion is that oligomers exhibit SDS-stable oligomeric bands on SDS−PAGE gels (*25*−*27*). From this criterion, it is clear that oligomers are formed much more readily from Aβ(1−42) than from Aβ(1−40) (*17*, *25*).

One difficulty in correlating soluble Aβ aggregates formed in vitro with those formed in vivo is the high probability that cellular interfaces affect the aggregation rates and even the aggregate structures. Sphingolipid- and cholesterol-rich bilayer membranes known as lipid rafts appear to be especially important sites of Aβ aggregation. These rafts are found largely but not exclusively in cell membrane domains known as caveolae (*28*). The β- and γ-secretases that generate Aβ peptides from APP as well as the Aβ peptides themselves are concentrated in lipid rafts (*29*−*31*). In the Tg2576 transgenic mouse model of AD as well as in AD brains, Aβ was highly concentrated in lipid rafts (*12*). In contrast to extracellular amyloid fibrils, which were SDS-insoluble, virtually all the Aβ in lipid rafts was extracted by SDS and corresponded to dimeric bands on SDS−PAGE gels. Several groups have investigated interactions of Aβ with glycosphingolipids in vitro and found that G_{M1} ganglioside in micelles and in reconstituted liposomes that resemble lipid rafts promotes Aβ binding and β-structure (*32*−*34*). Other reports have focused on the features of interfaces that are important in Aβ aggregation and found that amphiphilic interactions and micellar-like Aβ structures may play a role (*35*−*37*). Amphiphilic molecules such as Aβ tend to accumulate at interfaces between water and air or nonpolar liquids (*38*), and an Aβ monolayer at an air−water interface did undergo a rapid and substantial increase in β-structure content compared to that of a similar Aβ incubation in bulk solution (*39*).

We have previously described two systems in which polar−nonpolar interfaces appear to promote aggregation of Aβ(1−40) into fibers rich in β-structure. In the first, addition of monomeric Aβ(1−40) to the upper aqueous phase of a quiescent buffer/chloroform two-phase system resulted in Aβ aggregate formation within hours (*40*). In the second system, 1−4% hexafluoro-2-propanol (HFIP) in buffer was shown to form microdroplets. In this system, Aβ(1−40) aggregated in just a few minutes without agitation, and the usual lag time for aggregation was abolished (*41*). Although these polar−nonpolar interfaces have dramatic effects on Aβ structure, it is unclear whether they have direct counterparts in vivo. Biological membranes are composed largely of phospholipids with polar headgroups. Aβ aggregation is promoted by anionic phospholipid/sphingolipid vesicles, but interactions of Aβ with these vesicles appear to be restricted to the polar headgroups without penetration of amphiphilic Aβ into the bilayer (*42*−*44*). To compare the aggregation of Aβ at an anionic micellar interface to aggregation at polar−nonpolar interfaces, we have investigated Aβ aggregation in sodium dodecyl sulfate (SDS). Although SDS is often viewed as a denaturant that destroys native protein conformation, it provides an anionic micellar interface that has been shown to accelerate the aggregation of Aβ(1−40) and Aβ(1−42) over a limited range of low SDS concentrations (*45*). In contrast, at concentrations well above the critical micelle concentration (CMC), SDS stabilizes the peptide in an α-helical structure that does not aggregate and is amenable to NMR structure determination (*46*, *47*). SDS is also of interest because SDS−PAGE is the technique most often used to identify endogenous soluble Aβ oligomers. However, the Aβ aggregate that produces these oligomers and the conditions under which SDS itself can induce their formation have not been investigated. The studies described here are a first step in defining the effects of SDS, not only on Aβ aggregation but also on the disaggregation of preformed Aβ aggregates. In this report, we determine the effects of a range of SDS concentrations on Aβ(1−40) aggregation and structure. We also describe striking differences in secondary structure but similarities in morphology along the Aβ(1−40) aggregation pathways in SDS and in dilute HFIP.

EXPERIMENTAL PROCEDURES

Materials. The Aβ(1−40) peptide was obtained from the Peptide Synthesis Facility at the Mayo Clinic (Rochester, MN). SDS, bovine serum albumin, and thioflavin T were procured from Sigma (St. Louis, MO). All other buffers and salts were obtained from Fisher Inc.

Preparation of Aβ Monomers. The lyophilized stock of the Aβ(1−40) peptide was stored at −80 °C (desiccated). Samples were reconstituted in 0.1 M Tris-HCl (pH 8.0) at final concentrations of ∼500−700 μM. Any preformed aggregates were removed by size exclusion chromatography on Superdex 75, and concentrations of monomeric Aβ (*41*) were determined by UV absorbance with a calculated extinction coefficient of 1450 cm^{-1} M^{-1} at 276 nm (*24*).

Aggregation Reactions. All reactions and measurements were carried out at room temperature (25 °C). SDS stock solutions were filtered (0.2 μm cellulose acetate filters, VWR Scientific Products, West Chester, PA) and in some cases were sonicated (30 s) in a bath sonicator 20 min prior to being mixed with Aβ. Reactions were initiated in siliconized Eppendorf tubes by incubating appropriate concentrations of freshly purified Aβ(1−40) monomer in buffer in the presence or absence of SDS without agitation. The buffer consisted of 5 mM Tris-HCl and 50 mM NaCl (pH 8.0) for all reactions, except that 50 mM NaF replaced 50 mM NaCl for CD measurements with 100 μM Aβ to prevent high far-UV absorbance from NaCl (*33*). Direct comparison of 100 μM Aβ in 50 mM NaF and 50 mM NaCl showed no difference in aggregation rate as measured by thioflavin T fluorescence or in the rates of conversion to β-structure as measured by CD spectra above 205 nm. In some CD measurements, an aliquot of the initial mixture was transferred to the CD cuvette and left undisturbed for the remaining measurements to eliminate agitation resulting from

repeated pipetting of the sample. Aggregation kinetic parameters were obtained by monitoring the reaction with thioflavin T and fitting fluorescence (F) data points to the sigmoidal curve in eq 1 (*48*) using Origin 5.0.

$$F = \frac{a}{1 + e^{-[(t-t_{0.5})/b]}} \quad (1)$$

where t is time, a and b are fixed parameters, and $t_{0.5}$ is the time to reach half-maximal thioflavin T fluorescence. Data points were unweighted. Lag times were defined as described in ref *48* and were equal to $t_{0.5} - 2b$ for each fitted curve.

Protofibrils of Aβ(1−40) were prepared essentially as outlined previously (*24*, *40*). In brief, SEC-purified monomeric Aβ(1−40) (100−140 μM) was incubated in 10 mM Tris-HCl and 20 mM NaCl (pH 8.0) and agitated vigorously by continued vortexing to promote aggregation. After 16 h, the sample was centrifuged for 10 min in a microfuge (Beckman Coulter) at 18000*g*. The supernatant was chromatographed on a 1 cm × 30 cm Superdex 75 HR 10/30 column (Amersham Pharmacia) equilibrated in 20 mM Tris-HCl (pH 8.0), and Aβ eluting in the void volume was defined as the protofibril fraction (*24*). In some experiments, isolated protofibrils (2 μM) were elongated by incubation with purified monomeric Aβ(1−40) (50 μM) for 16 h (*24*). During the elongation reaction, the thioflavin T fluorescence increased at least 5-fold.

Dynamic Light Scattering (DLS). Hydrodynamic radius (R_H) measurements were made with a DynaPro MSX instrument (Protein Solutions Inc., Piscastaway, NJ) containing a gallium aluminum arsenide laser. The total light scattering intensity at a 90° angle in kilocounts per second was collected for samples (60 μL) in the quartz cuvette using an acquisition time of 5 s. Particle translation diffusion coefficients (D_T) were calculated from autocorrelation data and converted into R_H values with the Strokes−Einstein equation using the built-in Dynamics data analysis software provided by the manufacturer.

Circular Dichroism Spectroscopy. CD spectra were obtained in the far-UV region with a Jasco J-810 spectropolarimeter (Jasco Inc., Easton, MD) in continuous scan mode (260−190 nm) and a 0.1 cm path length quartz cuvette (Hellma). The acquisition parameters were 50 nm/min with response times of 8 s, a bandwidth of 1 nm, and a data pitch of 0.1 nm, and data sets were averaged over three scans unless otherwise noted. Spectra of appropriate solvent blanks were subtracted from the data sets. The corrected, averaged spectra were smoothed using the "means-movement" algorithm with a convolution width of 25 in the Jasco spectra analysis program. Data were normalized to mean residue ellipticity using the equation $[\theta] = [\theta]_{obs}(MRW/10lc)$, where MRW is the mean residue molecular weight of Aβ(1−40) (4331 g/mol divided by 40 residues), l is the optical path length (centimeters), and c is the concentration (grams per cubic centimeter). In some CD experiments with high concentrations of Aβ peptide, NaF was used in place of NaCl to reduce the noise in the far-UV region (*33*).

Fluorescence Spectroscopy. Thioflavin T fluorescence measurements were performed as described previously (*24*, *49*). Briefly, the fluorescence (F) was monitored in a microcuvette with a Perkin-Elmer LS-50B luminescence spectrometer after 15- or 30-fold dilution of Aβ(1−40) samples into 5 mM Tris-HCl (pH 8.0) containing 5 μM thioflavin T. Continuous measurements of F were taken for 10−15 min with the excitation wavelength fixed at 450 nm, the emission fixed at 480 nm, and the excitation and emission slits set at 10 nm, and the average F value was determined. The fluorescence of solvent blanks was subtracted.

Electron Microscopy (EM). Samples of Aβ aggregates were applied to 200 mesh Formvar-coated copper grids (Ernest F. Fullam, Inc., Latham, NY) and incubated for 10−15 min at room temperature. We then wicked off the sample with lens paper, washed it briefly by placing the grid face down on a droplet of water, and stained it by transferring the grid face down to a droplet of 2% uranyl acetate (Polysciences, Inc., Warrington, PA) for 5−10 min before wicking off the solution and air-drying. Grids were visualized in a Philips EM208S transmission electron microscope. To estimate widths of individual fibers, digital electron micrographs were analyzed by MCID Elite (MicroComputing Imaging Device 7.0, revision 1.0; Imaging Research, Inc.). Using the standard sample analysis menu and the "2 pt length" option, widths were measured at several places along numerous fibers from different images.

RESULTS

Aggregation of Aβ(1−40) Is Accelerated over a Very Narrow Range of SDS Concentrations. Monomeric Aβ(1−40) was purified by size exclusion chromatography to ensure removal of any preexisting aggregates. The time course of its aggregation was conveniently monitored with thioflavin T, a fluorophore that shows greatly enhanced fluorescence on binding to amyloid fibrils (*49*) and certain other Aβ aggregates enriched in β-structure (*41*). As reported previously (*45*), the addition of SDS accelerated aggregation over a narrow range of SDS concentrations (Figure 1A,B). The maximal rate with 100 μM Aβ(1−40) in Figure 1B was observed at 2 mM SDS, but it depended more on the CMC than on the absolute concentration of SDS. The CMC of SDS is 8 mM (0.22%, w/v) in water, but the addition of salt lowers the CMC (*50*). We examined several combinations of SDS and NaCl concentrations and found that 2 mM SDS in buffered 50 mM NaCl was slightly above the CMC. Formation of micelles with a hydrodynamic radius (R_H) of ∼2.0 nm was confirmed using DLS. However, the binding of SDS to Aβ(1−40) at a level of at least 0.4 g of SDS/g of protein (*51*) would imply that about a third of the SDS in the 2 mM SDS reaction in Figure 1 is bound to Aβ(1−40), thereby dropping the concentration of monomeric SDS below its nominal CMC. This point is considered further in the Discussion.

Secondary Structure Changes during Aβ Aggregation in the Presence of SDS. The secondary structure of Aβ(1−40) during incubations such as those in Figure 1B was analyzed by CD spectroscopy. The initial spectra for monomeric Aβ in the absence of SDS and with 0.5 mM SDS, a concentration well below its CMC, showed no minima above 200 nm and were consistent with previous reports of a largely random coil conformation in aqueous buffers prior to aggregation (data not shown; *42*, *52*). Over the 12 day incubation period, the amplitude of the spectra for these samples decreased by ∼50% (Figure 1C), suggesting that some process was removing monomeric Aβ(1−40) from solution. However,

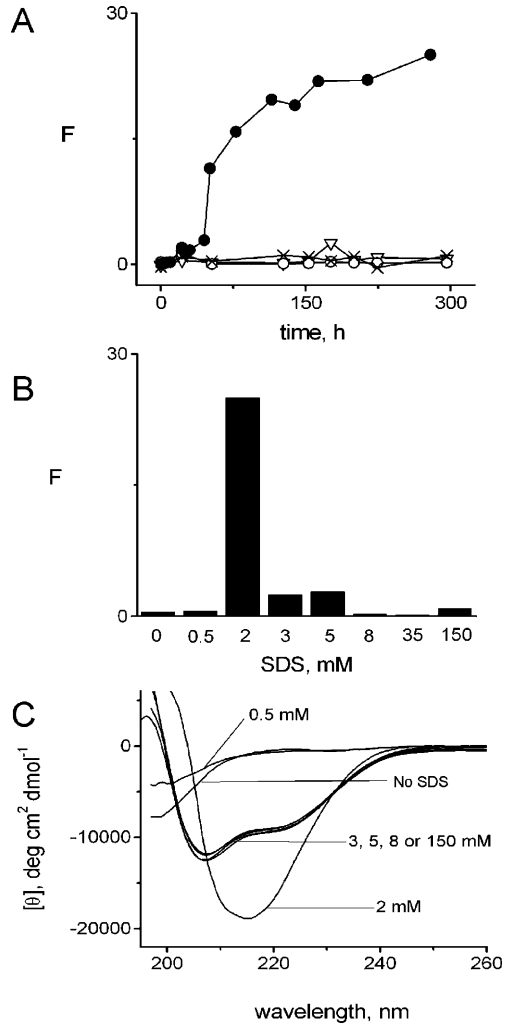

FIGURE 1: Dependence of Aβ(1−40) aggregation on the SDS concentration as monitored by thioflavin T fluorescence. Monomeric Aβ(1−40) (100 μM) was incubated in buffer [5 mM Tris-HCl and 50 mM NaCl (pH 8.0)] with the following concentrations of SDS: 0.5 (▽), 2.0 (●), 8.0 (○), and 150 mM (×). (A) At the indicated times, aliquots were diluted 30-fold for measurement of thioflavin T fluorescence. (B) Fluorescence intensities at 290 h from panel A as well as from additional reactions run in parallel under identical conditions in 3 and 5 mM SDS (240 h) and in 35 mM SDS or in the absence of SDS (290 h). (C) Aggregation reactions with 100 μM Aβ(1−40) in 5 mM Tris-HCl, 50 mM NaF (pH 8.0), and the indicated concentrations of SDS were left undisturbed in a CD cuvette. CD spectra were recorded at 290 h. Similar data were obtained in three replicate experiments.

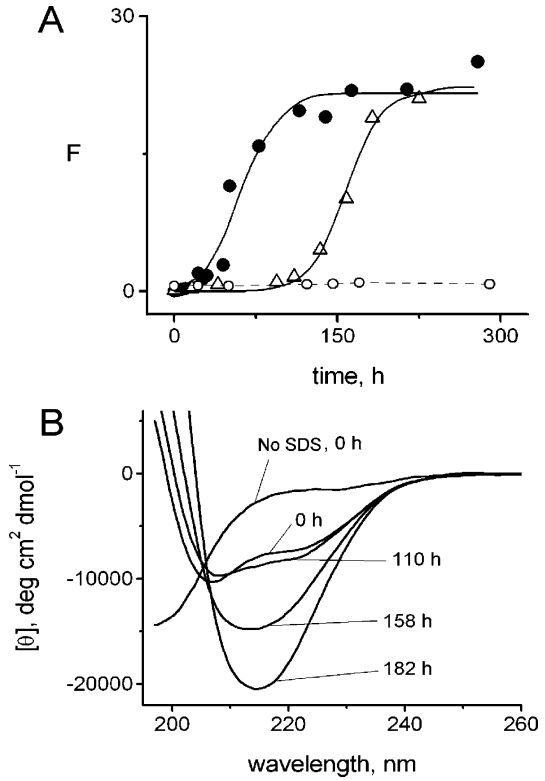

FIGURE 2: Correlation of Aβ(1−40) aggregation in SDS with secondary structure changes indicated by CD. (A) Monomeric Aβ-(1−40), at 100 (● and ○) or 25 μM (△), was incubated in the presence (● and △) or absence (○) of 2 mM SDS in buffered NaCl. At the indicated times, aliquots of the 25 μM Aβ(1−40) reaction mixture were diluted 15-fold into thioflavin T, and the fluorescence (F) was measured as described in the legend of Figure 1A. Points (●) are from Figure 1A. Values of F with 100 and 25 μM Aβ in 2 mM SDS were fit to eq 1 (solid lines) to give calculated lag times of 31 ± 5 and 125 ± 4 h, respectively. (B) Aliquots of the reaction mixture involving 25 μM Aβ in panel A were transferred to a CD cuvette, and CD spectra were recorded at each time point in panel A. Representative spectra are shown for the indicated times. The control spectrum is for 25 μM Aβ in buffered NaCl in the absence of SDS.

in the absence of SDS, we saw no indication of an initial transition from random coil to α-helical structure prior to aggregation, as observed in one report (*53*). In contrast, a rapid spectral change was obtained with samples in high concentrations of SDS (8, 35, and 150 mM). The CD spectrum for monomeric Aβ(1−40) was immediately altered with minima near 208 and 222 nm (Figure 1C), indicating formation of a substantial amount of α-helical structure (*54*). The spectra of these samples remained unchanged in shape throughout the incubation, although the amplitude for the sample in 150 mM SDS increased 10−15% at 290 h. CD spectra for the sample in 2 mM SDS showed a series of changes (described below) that were completed by 290 h. The spectrum at this point (Figure 1C) showed a minimum at 216 nm expected for a preponderance of β-structure (sheet and turn) as reported previously for Aβ fibrils (*55*) and protofibrils (*18*) generated in vitro.

The aggregation of 25 μM Aβ(1−40) in 2 mM SDS and buffered 50 mM NaCl was slower than that of 100 μM Aβ (Figure 2A). As expected for a nucleation-dependent aggregation process (*56*), both aggregation reactions displayed a lag phase prior to the onset of aggregation. However, the lag times were reduced from weeks to days by the addition of 2 mM SDS (Figure 2A). Changes in secondary structure of Aβ during these aggregation reactions were analyzed by CD spectroscopy, as shown for 25 μM Aβ(1−40) in 2 mM SDS in Figure 2B. A spectral shift indicating conversion to a predominant α-helical structure was evident immediately after addition of Aβ to 2 mM SDS. The shape and amplitude of the spectrum were similar to those obtained at higher SDS concentrations in Figure 1C, and this spectrum also remained unchanged for points taken over the first 40 h of the aggregation. However, a small shift became apparent at 110 h, the time in Figure 2A when aliquots from the 25 μM Aβ reaction first showed a slight increase in thioflavin T fluorescence. By 182 h, the shift in the CD spectrum became quite pronounced and indicated a preponderance of β-structure. This point corresponds to the time near maximal

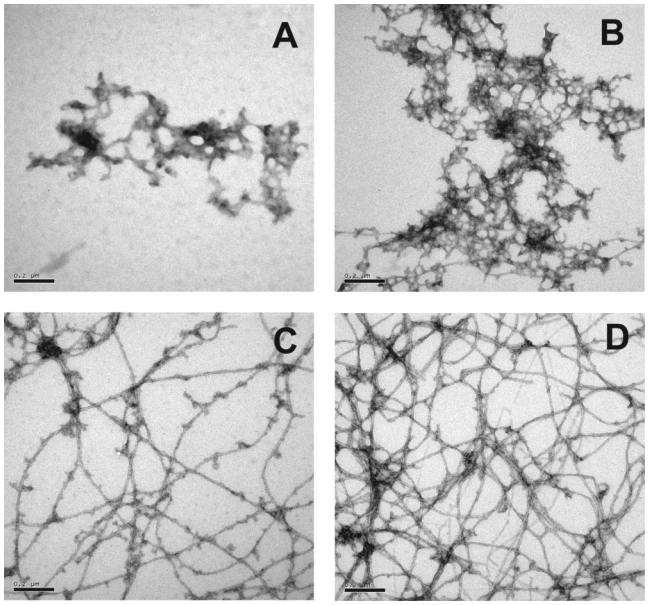

FIGURE 3: Electron micrographs of Aβ(1−40) aggregates formed after incubation in SDS for various amounts of time. Aliquots (10 μL) from the reaction mixture with 25 μM Aβ(1−40) and 2 mM SDS in panels A and B of Figure 2 were processed for negative staining and EM at the following times: (A) 0, (B) 40, (C) 100, and (D) 156 h. Widths of individual fibers in panel D averaged 11.8 ± 2.1 nm (SD, n = 148). Images are shown relative to a calibration bar of 200 nm.

thioflavin T fluorescence for this reaction in Figure 2A. The CD spectra in Figure 2B did not exhibit a precise isodichroic point but showed intersections of spectra between 204 and 210 nm, suggesting a system of more than two components with contributions from random coil, α-helix, and β-structure conformations. When the 182 h sample was centrifuged at 18000*g* for 10 min, more than 90% of the peptide remained in the supernatant as measured by CD and thioflavin T fluorescence (data not shown). Therefore, the Aβ(1−40) aggregates generated by prolonged incubation in 2 mM SDS are soluble.

Changes in Morphology during Aβ Aggregation in the Presence of SDS. To gain more insight into the structural changes occurring when Aβ(1−40) is mixed with SDS, samples taken from aggregation reactions were negatively stained with uranyl acetate and examined by EM. In Figure 3, samples were taken from the same 25 μM Aβ aggregation reaction mixture and at some of the same time points examined in Figure 2A to better compare aggregation rates and secondary structure with aggregate morphology. Immediately after addition of Aβ(1−40) to the 2 mM SDS solution, a relatively sparse number of amorphous clusters were observed with little indication of fibrous elements (Figure 3A). After 40 h, these clusters had developed into more extensive ordered latticelike structures and had become more numerous (Figure 3B). However, at this 40 h point, these structures did not yet generate thioflavin T fluorescence (Figure 2A) or show any change from the initial CD spectra that indicated partial α-helical structure. After 100 h (Figure 3C), most of the latticelike structures had evolved into a network of more distinct fibers, with numerous long fibers to which many knobs and short fibers were attached. At this time, the reaction was just beginning to produce aggregates that gave thioflavin T fluorescence (Figure 2A), and the CD spectra indicated a small component of β-structure in addition to the initial α-helical conformation. The final EM sample was taken at 156 h, and the number of fibers had significantly increased. This correlated well with substantial increases in the levels of aggregates that gave thioflavin T fluorescence and β-structure by CD (Figure 2A,B). Furthermore, the fibers at 156 h appeared to have matured to a form more typical of amyloid fibrils, with smoother features and few branching elements. The fiber widths at 156 h averaged 12 nm, somewhat larger than the 8−9 nm widths reported for elongated Aβ(1−40) protofibrils in the absence of SDS (*21*, *24*) but within the 7−12 nm range generally observed for amyloid fibrils (*57*).

Stability of Aβ Aggregates Formed in SDS. As noted in the introductory section, Aβ aggregates are produced at polar−nonpolar interfaces formed by microdroplets in dilute HFIP. These aggregates are rich in β-structure but initially are very unstable. When briefly incubated and then diluted out of HFIP, they dissaggregated completely within 2 min (*41*). The aggregates stabilized during a 10 day incubation in 2% HFIP, and dilution then induced only slight disaggregation over 1 h. To examine the stability of Aβ(1−40) aggregates formed in SDS, we disrupted the peptide-bound SDS micelles simply by 10-fold dilution of samples aggregated in 2 mM SDS. This dilution reduced the SDS concentration to well below its CMC. We anticipated that removal of SDS micelles would cause unstable Aβ structures to revert to conformations in which they are stable in the absence of SDS, while structures stable in both the presence and absence of SDS would persist.

CD, thioflavin T fluorescence, and EM were employed to monitor changes that occurred during dilution. To ensure that there was sufficient peptide for examination of the diluted samples, we focused on the mixture of 100 μM Aβ(1−40) in 2 mM SDS from Figure 1A. The secondary structure changes measured by CD during this reaction were similar to those observed in Figure 2B for 25 μM Aβ(1−40). Prior to dilution, the initial spectrum showed structure enriched in α-helix, but subsequent spectra showed a steady increase in β-structure content (Figure 4A) which was 2−3-fold faster than that in Figure 2B. In some replicates of this 100 μM Aβ(1−40) incubation, a spectrum consistent with β-structure was evident even at the earliest time point. Disruption of the SDS micelles by dilution resulted in an immediate reversion of the initial α-helical structure to random coil (0 h in Figure 4C), indicating that the α-helix was very unstable in the absence of SDS micelles. A slight shift toward β-structure was apparent after 6 h in the undiluted sample in Figure 4A, and the diluted sample showed a similar percentage conversion to β-structure (Figure 4B,C). The similarity indicated that the β-structure was largely stable in the absence of SDS micelles as soon as it was formed. The stability of the diluted β-structure aggregates was also monitored with thioflavin T, and an increase in fluorescence with time was observed (Figure 4D). The fluorescence intensities remained stable and showed no significant decay over the 1 h observation period. At early time points, the fluorescence lagged slightly behind the increase in β-structure content observed by CD (Figure 4C), suggesting that the initial β-structures may induce less enhancement of thioflavin T fluorescence.

EM analysis of 100 μM Aβ(1−40) in buffered 2 mM SDS revealed immediate formation of amorphous clusters, as

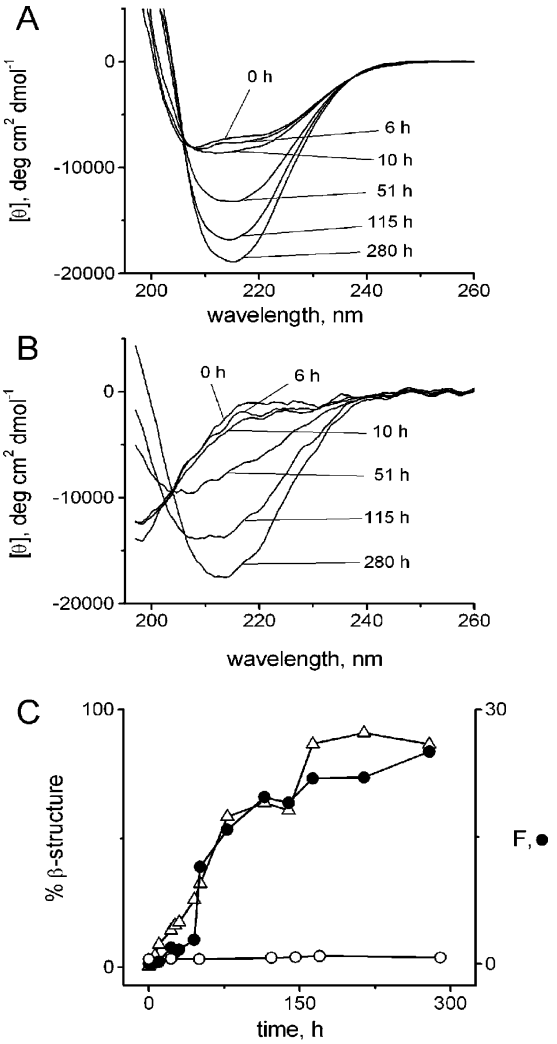

FIGURE 4: Stability of Aβ(1−40) aggregates formed in SDS after disruption of SDS micelles. Data were obtained from aggregation reactions with 100 μM Aβ(1−40) and buffered salt in 2 mM SDS. (A) The reaction in Figure 1C was left undisturbed in a CD cuvette, and CD spectra were recorded at the indicated times. (B) Samples from the reaction in Figure 1A were diluted 10-fold with buffered NaCl at the indicated times, and CD spectra were immediately recorded. Each trace is the average of six spectra. (C) The percentage of Aβ converted to β-structure in samples diluted as in panel B (% β-structure; △) was calculated from CD measurements of θ at 217 nm as $100(\theta_t - \theta_0)/(\theta_{280} - \theta_0)$, where subscripts refer to time points (t) in hours. Samples were also diluted 30-fold in parallel into 5 μM thioflavin T for measurement of fluorescence (F) (●, points from Figure 2A). The percentage conversion of CD spectra of the diluted control reaction mixture from Figure 2A was calculated assuming the same value of θ_{280} (○).

observed with the 25 μM Aβ incubation in Figure 3A. However, controls with bovine serum albumin in 2 mM SDS and Aβ in higher concentrations of SDS indicated that these clusters were also formed with other proteins when the SDS concentration was above the CMC. Panels A and B of Figure 5 compare images of albumin and Aβ in 2 mM SDS at equivalent concentrations by weight and at low magnification. The images are virtually indistinguishable, with many amorphous clusters that were not evident when either the protein or SDS was omitted. In this sample with albumin or with Aβ in 8 and 35 mM SDS, this morphology remained unchanged for up to 75 h (data not shown). With Aβ in 2 mM SDS, however, fibers began to emerge (Figure 5C) at

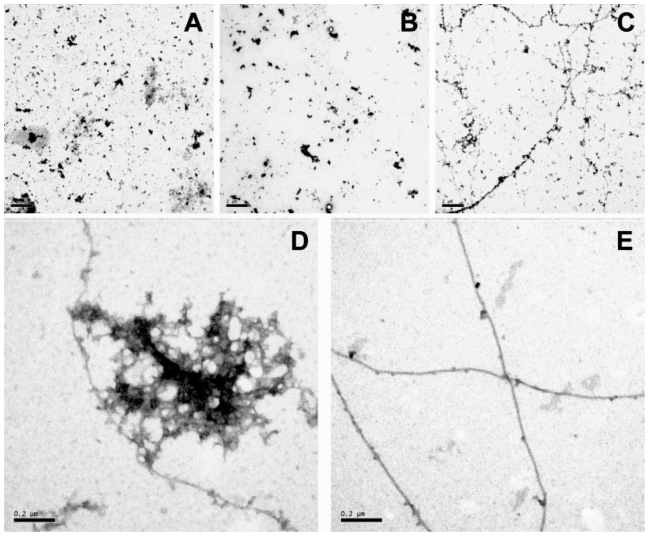

FIGURE 5: Electron micrographs of aggregates formed by bovine serum albumin and Aβ(1−40) in SDS and stability of aggregates after disruption of SDS micelles. Albumin (0.43 mg/mL) and Aβ-(1−40) (100 μM, 0.43 mg/mL) in buffered NaCl were incubated in 2 mM SDS. After various times, 10 μL aliquots of samples were taken for negative staining and EM: albumin after 6 h (A) and Aβ after 0 (B) and 6 h (C). The Aβ sample at 6 h was diluted 10-fold into buffered NaCl with (D) or without (E) 2 mM SDS, and 10 μL aliquots were taken for EM. Images are shown relative to calibration bars of 2 (A−C) or 0.2 μm (D and E).

the 6 h point when CD changes were detected in Figure 4A. Dilution of this sample into 2 mM SDS did not affect the morphology of either the amorphous aggregates or the fibers (Figure 5D), indicating that both structures were at least moderately stable in the continued presence of SDS micelles. On the other hand, dilution of this sample into buffer without SDS resulted in the loss of all the amorphous aggregates but retention of the fibers (Figure 5E). Some of the knobs or short appendages associated with the fibers also seemed to disappear on dilution. Ten-fold dilution of albumin in 2 mM SDS also resulted in the loss of all amorphous aggregates, further supporting the conclusion that these structures disaggregate in the absence of SDS micelles.

Slow Disaggregation of Aβ Protofibrils at High SDS Concentrations. The predominant conformation of monomeric Aβ(1−40) in concentrations of SDS above 3 mM remained α-helical for at least 12 days (Figure 1C). To determine whether this conformation is more stable than the β-structure adopted by fibrillar Aβ(1−40) at these concentrations of SDS, we isolated Aβ(1−40) protofibrils as we had reported previously (*24*, *41*). As noted in the introductory section, these soluble Aβ aggregates are composed of globules and short rods by EM, show primarily β-structure by CD, enhance the fluorescence of bound thioflavin T, and readily seed the growth of long fibrils. They are also very stable and showed no tendency to disaggregate over several hours in aqueous buffers without SDS (*41*). When Aβ(1−40) protofibrils were incubated in buffered 35 mM SDS, they also displayed no immediate change in secondary structure. Their CD spectrum exhibited a negative minimum at 219 nm, near the minimum characteristic of β-structure (Figure 6A). However, after 2 h, the spectrum showed a decrease in intensity at 219 nm and a relative increase in intensity at 208 nm. This trend gradually continued, and at 50 h, the spectrum indicated a conversion to predominant α-helical

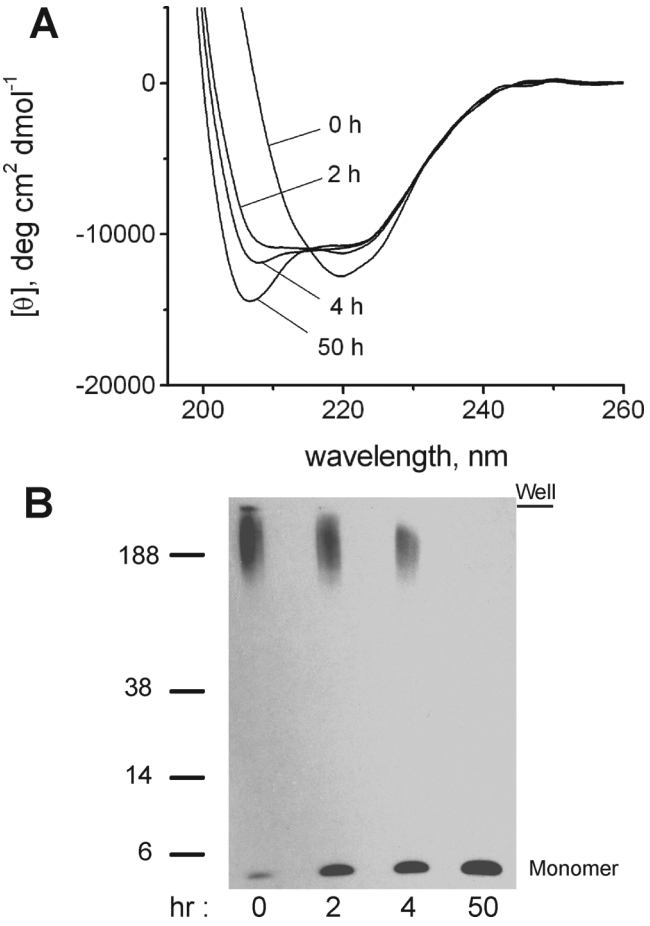

FIGURE 6: Dissolution of Aβ(1−40) protofibrils by high concentrations of SDS. (A) Freshly isolated Aβ protofibrils (10 μM) were incubated in 35 mM (1.0%) SDS in buffered NaCl, and CD spectra of the sample were taken at the indicated times. (B) Aliquots of the freshly isolated Aβ protofibrils in panel A were transferred to 1.0% SDS and incubated for the indicated times. Samples (20 μL, 20 pmol) were applied to a 4−12% bis-Tris gel (NuPAGE, Invitrogen Inc., Carlsbad, CA), electrophoresed in NuPAGE MES SDS running buffer that contained 0.1% SDS, and immunoblotted on Immobilon-P. The transfers to SDS were timed so that all samples were run on SDS−PAGE immediately after the incubation. The gel was calibrated with dye-linked M_W markers (SeeBlue Plus2 Prestained Standards, Invitrogen), and the blot was probed using monoclonal antibody 6E10 with ECL development. Similar results were obtained with isolated Aβ(1−40) protofibrils that had been elongated.

structure with a minimum at 208 nm and a shoulder at 220 nm. The superimposed spectra exhibited a well-defined isodichroic point at ~214 nm (Figure 6A), suggesting that the conversion of β- to α-helical structure involved a two-state process without significant accumulation of other intermediates. The Aβ protofibril incubation in 35 mM SDS was also monitored by SDS−PAGE and Western blotting. Three Aβ species were detected immediately after addition of SDS: 4 kDa monomer near the gel dye front, aggregate that remained in the loading well, and more diffuse aggregate that barely entered the separation gel (Figure 6B, 0 h). Such large aggregates are consistent with our previous estimate that the minimum M_W for these Aβ protofibrils is ~7×10^3 kDa (*24*). Protofibril samples were incubated in SDS for longer times that corresponded to the times at which the CD spectra were taken. These samples showed progressive conversion of aggregates to monomer over the 50 h interval (Figure 6B). Therefore, the shift in conformation from β- to α-helical structure observed by CD was accompanied by an increasing level of disaggregation of the protofibrils as measured by SDS−PAGE. It is noteworthy that protofibril stocks showed some variability in these experiments. SDS−PAGE analysis of some preparations gave only two species, monomer and aggregate in the loading well. Furthermore, protofibril preparations that had been aged by incubation at room temperature for several days showed slower rates of conversion to α-helical structure on addition of SDS when analyzed as in Figure 6. This increasing stability to SDS-induced disaggregation supports our previous report that incubation of Aβ protofibrils results in progressive resistance to disaggregation in general (*41*).

DISCUSSION

The Acceleration of Aβ(1−40) Aggregation by SDS Requires a High Ratio of Peptide to Bound Micellar SDS. In this study, the aggregation of Aβ(1−40) was stimulated by SDS but only over a narrow range of SDS concentrations. The rate of Aβ aggregation to fibrils was increased at 2 mM SDS, a concentration near its CMC in our experiments, but not at SDS concentrations that were 4-fold higher or lower (Figure 1A,B). Similar effects of SDS on the aggregation of Aβ(1−40) and Aβ(1−42) were previously reported by Yamamoto et al. (*45*), and the aggregation of other amyloidogenic proteins also showed a comparable dependence on SDS concentration. In one example, a peptide corresponding to residues 18−34 from the SCR3 domain of the human complement receptor slowly converted from a random coil conformation to fibrils rich in β-structure over a period of several days in the absence of SDS (*58*). In 20 mM SDS, spectra characteristic of an α-helical conformation remained effectively unchanged for more than 2 days. However, in 3 mM SDS, a concentration slightly below the CMC in their experiments, spectra that initially indicated a predominantly α-helical structure gradually shifted over a few hours to a curve typical of β-structure and fibrils were produced (*58*). Effects of SDS consistent with these observations also were made with amyloid fibrils prepared from β_2-microglobulin (*59*). SDS over a narrow range of concentrations just below the CMC accelerated the extension of fibril seeds and stabilized the extended fibrils, while higher SDS concentrations disaggregated the fibrils to a structure rich in α-helix.

Concentrations of SDS that induce the formation of α-helical structure by Aβ(1−40) also give rise to SDS micelles. No conversion to α-helix was observed at 0.5 mM SDS, and no micelles were observed by DLS; on the other hand, all SDS concentrations of ≥2 mM resulted in the immediate appearance of α-helix. The unique effect of SDS concentrations near the CMC in promoting amyloid fibril formation can be explained in the context of classic measurements of SDS binding by proteins. Several proteins bound SDS at plateau levels of ~0.4 g of SDS/g of protein just below the CMC and ~1.4 g/g of protein above the CMC (*51*). Proteins stabilized the bound SDS in the form of micelles even at SDS concentrations that were slightly below the CMC in the absence of proteins (*60*), but the micelles formed at the lower SDS concentrations were smaller (*61*). A level of 0.4 g of bound SDS/g of Aβ(1−40) corresponds to approximately six molecules of SDS per peptide, a value considerably lower than the minimum number of ~30 SDS

molecules per micelle measured for SDS micelles bound to bovine serum albumin (*62*). The difference suggests that more than one Aβ peptide binds to a single SDS micelle at SDS concentrations just below the CMC, and the intermolecular proximity of these peptides in turn could promote formation of aggregates rich in β-structure. This proximity effect is likely to contribute to differences in the rates of formation of β-structured aggregates with Aβ concentration. Reducing the Aβ(1−40) concentration from 100 to 25 μM in the presence of 2 mM SDS increased the lag time for Aβ aggregation by a factor of 4 (Figure 2A). While this decrease in aggregation rate is consistent with a simple mass-action effect at the lower Aβ concentration, it also is likely to result from a smaller ratio of Aβ peptides per SDS micelle.

At concentrations of SDS well above the CMC, the larger SDS micelles that are bound to Aβ(1−40) may be more compact (*61*) and are more effective in stabilizing α-helical structure. For example, Aβ(1−40) protofibrils are rich in β-structure and extremely stable in the absence of SDS (*41*), but they were slowly converted to a monomeric form with increased α-helical structure content upon addition of SDS to 35 mM (1%), a concentration typically used to prepare samples for SDS−PAGE (Figure 6). This structure in association with these micelles thus is more stable than fibrillar Aβ, an observation that explains why the initial α-helical structure formed upon addition of high concentrations of SDS to monomeric Aβ did not proceed to fibers. However, this stability was lost if the micelles were removed. Addition of Aβ(1−40) to 2 mM SDS initially gave a preponderance of α-helical structure, but this structure reverted to random coil upon removal of the micelles by dilution to well below the CMC (Figure 4B). Furthermore, amorphous aggregates, which were apparent by EM when either bovine serum albumin or Aβ(1−40) interacted with the micelles, immediately disappeared when SDS was diluted to well below its CMC (Figure 5A,B). Although these amorphous aggregates may reflect only the small percentage of protein−SDS complexes large enough to be detected by EM, they presumably assume the same α-helical structure observed by CD with the bulk solutions. Their disappearance on dilution supported a loss of this structure on removal of the micelles. In contrast, the earliest Aβ fibers formed in 2 mM SDS did not require the support of micelles for stability and remained after dilution (Figure 5E).

The Interfacial Formation of Fibrillar Aβ Depends on Peptide Proximity but Not on Initial Peptide Conformation. As noted in the introductory section, current interest in small soluble Aβ aggregates that are formed in vivo is high because they are proposed to be neurotoxic and to initiate neurodegeneration. The aggregates of Aβ(1−40) generated at the polar−nonpolar interface in dilute HFIP and at the anionic micellar interface in 2 mM SDS are not sedimented by centrifugation at 18000*g* for 10 min, even after several days when fibers have become apparent by EM, and thus are classified as soluble. These fibers thus share many features with protofibrils, although they are not identical to protofibrils because they seed the aggregation of Aβ(1−40) monomers ineffectively: The Aβ(1−40) fibers obtained after prolonged incubation in dilute HFIP elongated only slightly following dilution into 60 μM Aβ(1−40) monomers (*41*), and similar dilution of Aβ(1−40) aggregates obtained after several days of incubation in 2 mM SDS into monomeric Aβ(1−40) resulted in elongation rates that were less than 10% of those obtained in parallel with isolated Aβ(1−40) protofibrils (data not shown). In both of these interfacial systems, changes in peptide secondary structure occurred immediately when Aβ was introduced. With dilute HFIP, the change involved conversion from random coil to a predominant β-structure. Furthermore, the conversion to β-structure was accompanied by a rapid increase in fluorescence in the presence of thioflavin T, a property usually thought to indicate the generation of an amyloid-like cross-β-structure. These features stood in sharp contrast to the initial Aβ structure formed in 2 mM SDS, which showed a partial α-helical conformation and gave no thioflavin T fluorescence. Despite these differences in initial secondary structure, the progressive changes in EM morphology that accompanied the development of fiber structures were strikingly similar both in buffered 2% HFIP and in 2 mM SDS (Figure 7). In both cases, amorphous clustered aggregates were immediately formed and evolved slightly into a mesh or lattice of fiberlike elements over a roughly 2 day period (Figure 7A,B) However, after a few more days in either 2% HFIP or 2

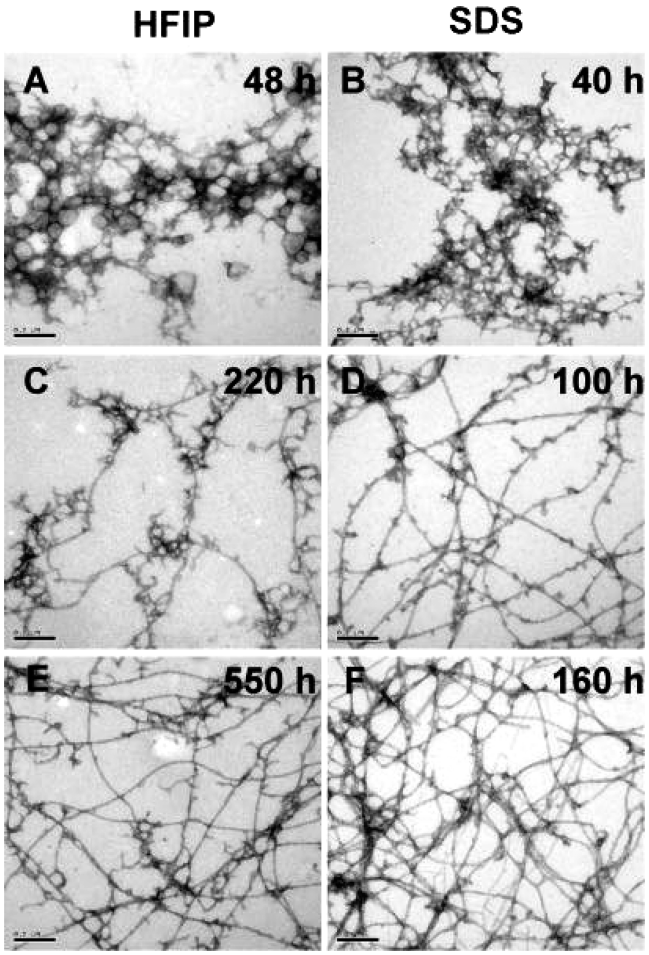

FIGURE 7: Similar progressive changes in morphology for interfacial Aβ(1−40) aggregates formed in 2% HFIP or 2 mM SDS. (A, C, and E) Monomeric Aβ(1−40) (40 μM) was incubated in 5 μM thioflavin T, 5 mM Tris-HCl (pH 8.0), and 2% HFIP at 23 °C (*41*). Aliquots of the solution were centrifuged at 18000*g* for 10 min at the indicated times, and supernatant samples (10 μL) were removed and processed for negative staining and EM. (B, D, and F) Images from the soluble reaction mixture with 25 μM Aβ(1−40) and 2 mM SDS in Figure 3 are shown here for comparison. All images are shown relative to a calibration bar of 200 nm.

mM SDS, Aβ began to show more distinct fibers, including long fibers from which many short fibers branched (Figure 7C,D). These fibers continued to mature over subsequent days to a form more typical of amyloid fibrils, as the number of branching elements decreased and the fibers became smoother (Figure 7E,F).

We suggest that two conclusions can be drawn from the facts that the initial secondary structures adopted by Aβ at the SDS micelle and the HFIP microdroplet interfaces were completely different and yet fibers emerged from latticelike matrices in both systems at approximately the same rates. First, neither the α-helical conformation induced at the SDS interface nor the β-structure rapidly formed at the HFIP interface appears to uniquely promote Aβ fiber formation. If one of these conformations served as an obligatory intermediate in, for example, an initial nucleation step, one would expect fiber formation to occur much more rapidly at the interface corresponding to this conformation. Second, both interfaces clearly accelerate fiber formation relative to the rate with buffer alone. Therefore, these interfaces provide a means of concentrating Aβ from the bulk solution in essentially a two-dimensional space, and aggregation appears to be enhanced simply by the greater likelihood that peptide molecules will come into contact.

REFERENCES

1. Cohen, A. S., and Calkins, E. (1959) Electron microscopic observation on a fibrous component in amyloid of diverse origins, *Nature 183*, 1202−1203.
2. Glenner, G. G., and Wong, C. W. (1984) Alzheimer's disease: Initial report of the purification and characterization of a novel cerebrovascular amyloid protein, *Biochem. Biophys. Res. Commun. 120*, 885−890.
3. Miller, D. L., Papayannopoulos, I. A., Styles, J., Bobin, S. A., Lin, Y. Y., Biemann, K., and Iqbal, K. (1993) Peptide compositions of the cerebrovascular and senile plaque core amyloid deposits of Alzheimer's disease, *Arch. Biochem. Biophys. 301*, 41−52.
4. Selkoe, D. J. (2001) Alzheimer's disease: Genes, proteins, and therapy, *Physiol. Rev. 81*, 741−766.
5. Hardy, J. A., and Higgins, G. A. (1992) Alzheimer's disease: The amyloid cascade hypothesis, *Science 256*, 184−185.
6. Selkoe, D. J., and Podlisny, M. B. (2002) Deciphering the genetic basis of Alzheimer's disease, *Annu. Rev. Genomics Hum. Genet. 3*, 67−99.
7. Nilsberth, C., Westlind-Danielsson, A., Eckman, C. B., Condron, M. M., Axelman, K., Forsell, C., Stenh, C., Luthman, J., Teplow, D. B., Younkin, S. G., Naslund, J., and Lannfelt, L. (2001) The 'Arctic' APP mutation (E693G) causes Alzheimer's disease by enhanced Aβ protofibril formation, *Nat. Neurosci. 4*, 887−893.
8. Hardy, J., and Selkoe, D. J. (2002) The amyloid hypothesis of Alzheimer's disease: Progress and problems on the road to therapeutics, *Science 297*, 353−356.
9. Hartley, D. M., Walsh, D. M., Ye, C. P., Diehl, T., Vasquez, S., Vassilev, P. M., Teplow, D. B., and Selkoe, D. J. (1999) Protofibrillar intermediates of amyloid β-protein induce acute electrophysiological changes and progressive neurotoxicity in cortical neurons, *J. Neurosci. 19*, 8876−8884.
10. Klein, W. L., Krafft, G. A., and Finch, C. E. (2001) Targeting small Aβ oligomers: The solution to an Alzheimer's disease conundrum? *Trends Neurosci. 24*, 219−224.
11. Westerman, M. A., Cooper-Blacketer, D., Mariash, A., Kotilinek, L., Kawarabayashi, T., Younkin, L. H., Carlson, G. A., Younkin, S. G., and Ashe, K. H. (2002) The relationship between Aβ and memory in the Tg2576 mouse model of Alzheimer's disease, *J. Neurosci. 22*, 1858−1867.
12. Kawarabayashi, T., Shoji, M., Younkin, L. H., Lin, W. L., Dickson, D. W., Murakami, T., Matsubara, E., Abe, K., Ashe, K. H., and Younkin, S. G. (2004) Dimeric amyloid β protein rapidly accumulates in lipid rafts followed by apolipoprotein E and phosphorylated tau accumulation in the Tg2576 mouse model of Alzheimer's disease, *J. Neurosci. 24*, 3801−3809.
13. McLean, C. A., Cherny, R. A., Fraser, F. W., Fuller, S. J., Smith, M. J., Beyreuther, K., Bush, A. I., and Masters, C. L. (1999) Soluble pool of Aβ amyloid as a determinant of severity of neurodegeneration in Alzheimer's disease, *Ann. Neurol. 46*, 860−866.
14. Podlisny, M. B., Ostaszewski, B. L., Squazzo, S. L., Koo, E. H., Rydell, R. E., Teplow, D. B., and Selkoe, D. J. (1995) Aggregation of secreted amyloid β-protein into sodium dodecyl sulfate-stable oligomers in cell culture, *J. Biol. Chem. 270*, 9564−9570.
15. Walsh, D. M., Klyubin, I., Fadeeva, J. V., Cullen, W. K., Anwyl, R., Wolfe, M. S., Rowan, M. J., and Selkoe, D. J. (2002) Naturally secreted oligomers of amyloid β protein potently inhibit hippocampal long-term potentiation *in vivo*, *Nature 416*, 535−539.
16. Cleary, J. P., Walsh, D. M., Hofmeister, J. J., Shankar, G. M., Kuskowski, M. A., Selkoe, D. J., and Ashe, K. H. (2005) Natural oligomers of the amyloid-β protein specifically disrupt cognitive function, *Nat. Neurosci. 8*, 79−84.
17. Walsh, D. M., Lomakin, A., Benedek, G. B., Condron, M. M., and Teplow, D. B. (1997) Amyloid β-protein fibrillogenesis: Detection of a protofibrillar intermediate, *J. Biol. Chem. 272*, 22364−22372.
18. Walsh, D. M., Hartley, D. M., Kusumoto, Y., Fezoui, Y., Condron, M. M., Lomakin, A., Benedek, G. B., Selkoe, D. J., and Teplow, D. B. (1999) Amyloid β-protein fibrillogenesis: Structure and biological activity of protofibrillar intermediates, *J. Biol. Chem. 274*, 25945−25952.
19. Harper, J. D., Wong, S. S., Lieber, C. M., and Lansbury, P. T., Jr. (1997) Observation of metastable Aβ amyloid protofibrils by atomic force microscopy, *Chem. Biol. 4*, 119−125.
20. Harper, J. D., Wong, S. S., Lieber, C. M., and Lansbury, P. T., Jr. (1999) Assembly of Aβ amyloid peptides: An *in vitro* model for a possible early event in Alzheimer's disease, *Biochemistry 38*, 8972−8980.
21. Goldsbury, C. S., Wirtz, S., Muller, S. A., Sunderji, S., Wicki, P., Aebi, U., and Frey, P. (2000) Studies on the *in vitro* assembly of Aβ 1−40: Implications for the search for Aβ fibril formation inhibitors, *J. Struct. Biol. 130*, 217−231.
22. Huang, T. H., Yang, D. S., Plaskos, N. P., Go, S., Yip, C. M., Fraser, P. E., and Chakrabartty, A. (2000) Structural studies of soluble oligomers of the Alzheimer β-amyloid peptide, *J. Mol. Biol. 297*, 73−87.
23. Dahlgren, K. N., Manelli, A. M., Stine, W. B., Jr., Baker, L. K., Krafft, G. A., and LaDu, M. J. (2002) Oligomeric and fibrillar species of amyloid-β peptides differentially affect neuronal viability, *J. Biol. Chem. 277*, 32046−32053.
24. Nichols, M. R., Moss, M. A., Reed, D. K., Lin, W.-L., Mukhopadhyay, R., Hoh, J. H., and Rosenberry, T. L. (2002) Growth of β-amyloid(1−40) protofibrils by monomer elongation and lateral association. Characterization of distinct products by light scattering and atomic force microscopy, *Biochemistry 41*, 6115−6127.
25. Lambert, M. P., Barlow, A. K., Chromy, B. A., Edwards, C., Freed, R., Liosatos, M., Morgan, T. E., Rozovsky, I., Trommer, B., Viola, K. L., Wals, P., Zhang, C., Finch, C. E., Krafft, G. A., and Klein, W. L. (1998) Diffusible, nonfibrillar ligands derived from $A\beta_{1-42}$ are potent central nervous system neurotoxins, *Proc. Natl. Acad. Sci. U.S.A. 95*, 6448−6453.
26. Chromy, B. A., Nowak, R. J., Lambert, M. P., Viola, K. L., Chang, L., Velasco, P. T., Jones, B. W., Fernandez, S. J., Lacor, P. N., Horowitz, P., Finch, C. E., Krafft, G. A., and Klein, W. L. (2003) Self-assembly of Aβ(1−42) into globular neurotoxins, *Biochemistry 42*, 12749−12760.
27. Stine, W. B. J., Dahlgren, K. N., Krafft, G. A., and LaDu, M. J. (2003) *In vitro* characterization of conditions for amyloid-β peptide oligomerization and fibrillogenesis, *J. Biol. Chem. 278*, 11612−11622.
28. Simons, K., and Vaz, W. L. (2004) Model systems, lipid rafts, and cell membranes, *Annu. Rev. Biophys. Biomol. Struct. 33*, 269−295.
29. Riddell, D. R., Christie, G., Hussain, I., and Dingwall, C. (2001) Compartmentalization of β-secretase (Asp2) into low-buoyant density, noncaveolar lipid rafts, *Curr. Biol. 11*, 1288−1293.
30. Wahrle, S., Das, P., Nyborg, A. C., McLendon, C., Shoji, M., Kawarabayashi, T., Younkin, L. H., Younkin, S. G., and Golde, T. E. (2002) Cholesterol-dependent γ-secretase activity in buoyant cholesterol-rich membrane microdomains, *Neurobiol. Dis. 9*, 11−23.

31. Lee, S. J., Liyanage, U., Bickel, P. E., Xia, W., Lansbury, P. T., Jr., and Kosik, K. S. (1998) A detergent-insoluble membrane compartment contains Aβ in vivo, *Nat. Med. 4*, 730−734.
32. Choo-Smith, L. P., Garzon-Rodriguez, W., Glabe, C. G., and Surewicz, W. K. (1997) Acceleration of amyloid fibril formation by specific binding of Aβ-(1−40) peptide to ganglioside-containing membrane vesicles, *J. Biol. Chem. 272*, 22987−22990.
33. Choo-Smith, L. P., and Surewicz, W. K. (1997) The interaction between Alzheimer amyloid β(1−40) peptide and ganglioside GM1-containing membranes, *FEBS Lett. 402*, 95−98.
34. Kakio, A., Nishimoto, S., Yanagisawa, K., Kozutsumi, Y., and Matsuzaki, K. (2002) Interactions of amyloid β-protein with various gangliosides in raft-like membranes: Importance of GM1 ganglioside-bound form as an endogenous seed for Alzheimer amyloid, *Biochemistry 41*, 7385−7390.
35. Lomakin, A., Chung, D. S., Benedek, G. B., Kirschner, D. A., and Teplow, D. B. (1996) On the nucleation and growth of amyloid β-protein fibrils: Detection of nuclei and quantification of rate constants, *Proc. Natl. Acad. Sci. U.S.A. 93*, 1125−1129.
36. Tjernberg, L. O., Pramanik, A., Bjorling, S., Thyberg, P., Thyberg, J., Nordstedt, C., Berndt, K. D., Terenius, L., and Rigler, R. (1999) Amyloid β-peptide polymerization studied using fluorescence correlation spectroscopy, *Chem. Biol. 6*, 53−62.
37. Yong, W., Lomakin, A., Kirkitadze, M. D., Teplow, D. B., Chen, S. H., and Benedek, G. B. (2001) Structure determination of micelle-like intermediates in amyloid β-protein fibril assembly by using small angle neutron scattering, *Proc. Natl. Acad. Sci. U.S.A. 99*, 150−154.
38. Pratt, L. R., and Pohorille, A. (2002) Hydrophobic effects and modeling of biophysical aqueous solution interfaces, *Chem. Rev. 102*, 2671−2692.
39. Schladitz, C., Vieira, E. P., Hermel, H., and Mohwald, H. (1999) Amyloid-β-sheet formation at the air−water interface, *Biophys. J. 77*, 3305−3310.
40. Nichols, M. R., Moss, M. A., Reed, D. K., Hoh, J. H., and Rosenberry, T. L. (2005) Rapid assembly of amyloid-β peptide at a liquid/liquid interface produces unstable β-sheet fibers, *Biochemistry 44*, 165−173.
41. Nichols, M. R., Moss, M. A., Reed, D. K., Cratic-McDaniel, S., Hoh, J. H., and Rosenberry, T. L. (2005) Amyloid-β protofibrils differ from amyloid-β aggregates induced in dilute hexafluoroisopropanol in stability and morphology, *J. Biol. Chem. 280*, 2471−2480.
42. Terzi, E., Holzemann, G., and Seelig, J. (1997) Interaction of Alzheimer β-amyloid peptide(1−40) with lipid membranes, *Biochemistry 36*, 14845−14852.
43. Matsuzaki, K., and Horikiri, C. (1999) Interactions of amyloid β-peptide(1−40) with ganglioside-containing membranes, *Biochemistry 38*, 4137−4142.
44. Yip, C. M., and McLaurin, J. (2001) Amyloid-β peptide assembly: A critical step in fibrillogenesis and membrane disruption, *Biophys. J. 80*, 1359−1371.
45. Yamamoto, N., Hasegawa, K., Matsuzaki, K., Naiki, H., and Yanagisawa, K. (2004) Environment- and mutation-dependent aggregation behavior of Alzheimer amyloid β-protein, *J. Neurochem. 90*, 62−69.
46. Coles, M., Bicknell, W., Watson, A. A., Fairlie, D. P., and Craik, D. J. (1998) Solution structure of amyloid β-peptide(1−40) in a water-micelle environment. Is the membrane-spanning domain where we think it is? *Biochemistry 37*, 11064−11077.
47. Shao, H., Jao, S., Ma, K., and Zagorski, M. G. (1999) Solution structures of micelle-bound amyloid β-(1−40) and β-(1−42) peptides of Alzheimer's disease, *J. Mol. Biol. 285*, 755−773.
48. Nielsen, L., Frokjaer, S., Brange, J., Uversky, V. N., and Fink, A. L. (2001) Probing the mechanism of insulin fibril formation with insulin mutants, *Biochemistry 40*, 8397−8409.
49. LeVine, H. (1993) Thioflavine T interaction with synthetic Alzheimer's disease β-amyloid peptides: Detection of amyloid aggregation in solution, *Protein Sci. 2*, 404−410.
50. Henry, G. D., and Sykes, B. D. (1994) Methods to study membrane protein structure in solution, *Methods Enzymol. 239*, 515−535.
51. Reynolds, J. A., and Tanford, C. (1970) The gross conformation of protein-sodium dodecyl sulfate complexes, *J. Biol. Chem. 245*, 5161−5165.
52. Gursky, O., and Aleshkov, S. (2000) Temperature-dependent β-sheet formation in β-amyloid Aβ_{1-40} peptide in water: Uncoupling β-structure folding from aggregation, *Biochim. Biophys. Acta 1476*, 93−102.
53. Kirkitadze, M. D., Condron, M. M., and Teplow, D. B. (2001) Identification and characterization of key kinetic intermediates in amyloid β-protein fibrillogenesis, *J. Mol. Biol. 312*, 1103−1119.
54. Barrow, C. J., Yasuda, A., Kenny, P. T., and Zagorski, M. G. (1992) Solution conformations and aggregational properties of synthetic amyloid β-peptides of Alzheimer's disease. Analysis of circular dichroism spectra, *J. Mol. Biol. 225*, 1075−1093.
55. Soto, C., and Frangione, B. (1995) Two conformational states of amyloid β-peptide: Implications for the pathogenesis of Alzheimer's disease, *Neurosci. Lett. 186*, 115−118.
56. Jarrett, J. T., and Lansbury, P. T., Jr. (1993) Seeding "one-dimensional crystallization" of amyloid: A pathogenic mechanism in Alzheimer's disease and scrapie? *Cell 73*, 1055−1058.
57. Makin, O. S., and Serpell, L. C. (2002) Examining the structure of the mature amyloid fibril, *Biochem. Soc. Trans. 30*, 521−525.
58. Pertinhez, T. A., Bouchard, M., Smith, R. A., Dobson, C. M., and Smith, L. J. (2002) Stimulation and inhibition of fibril formation by a peptide in the presence of different concentrations of SDS, *FEBS Lett. 529*, 193−197.
59. Yamamoto, S., Hasegawa, K., Yamaguchi, I., Tsutsumi, S., Kardos, J., Goto, Y., Gejyo, F., and Naiki, H. (2004) Low concentrations of sodium dodecyl sulfate induce the extension of β2-microglobulin-related amyloid fibrils at a neutral pH, *Biochemistry 43*, 11075−11082.
60. Daban, J. R., Samso, M., and Bartolome, S. (1991) Use of Nile red as a fluorescent probe for the study of the hydrophobic properties of protein-sodium dodecyl sulfate complexes in solution, *Anal. Biochem. 199*, 162−168.
61. Santos, S. F., Zanette, D., Fischer, H., and Itri, R. (2003) A systematic study of bovine serum albumin (BSA) and sodium dodecyl sulfate (SDS) interactions by surface tension and small-angle X-ray scattering, *J. Colloid Interface Sci. 262*, 400−408.
62. Turro, N. J., Lei, X. G., Ananthapadmanabhan, K. P., and Aronson, M. (1995) Spectroscopic probe analysis of protein-surfactant interactions: The BSA/SDS system, *Langmuir 11*, 2525−2533.

BI060323T